smoothness could result simply from averaging.

ACKNOWLEDGMENTS

The author gratefully acknowledges many very helpful, stimulating, and informative discussions with Professor C. G. Grenier. Special thanks are extended to Dr. J. O. Betterton, then of the Oak Ridge National Laboratory, for supplying the high-quality zirconium that made both this and the dHvA investigation possible.

*Work performed under the auspices of the U. S. Atomic Energy Commission and is AEC Report No. ORO-3087-49.

†Present address: Department of Physics and Astronomy, University of Kentucky, Lexington, Kentucky 40506.

[1]I. M. Lifshitz, M. Ya. Azbel, and M. I. Kaganov, Zh. Eksperim. i Teor. Fiz. 31, 63 (1956) [Sov. Phys. JETP 4, 41 (1957)].

[2]I. M. Lifshitz and V. G. Peschanskii, Zh. Eksperim. i Teor. Fiz. 35, 1251 (1958); 38, 188 (1960) [Sov. Phys. JETP 8, 875 (1959); 11, 137 (1960)].

[3]E. Fawcett, Phys. Rev. Letters 6, 534 (1961).

[4]S. L. Altmann and C. J. Bradley, Phys. Rev. 135, A1253 (1964); Proc. Phys. Soc. (London) 92, 764 (1967).

[5]References 4, 6, and 7 all used a four-integer system of Miller indices in which the reciprocal-lattice vectors were used as the basis vectors. The present investigations use the now standard system where the real-space lattice vectors are used as basis vectors. Thus the reciprocal-lattice-vector direction is given as $\langle 10\bar{1}0 \rangle$. In discussing trajectories, the direction in reciprocal or k space is always given.

[6]T. L. Loucks, Phys. Rev. 159, 544 (1967).

[7]A. C. Thorsen and A. S. Joseph, Phys. Rev. 131, 2078 (1963).

[8]C. G. Grenier (private communication).

[9]The author would like to thank R. G. Goodrich and J. M. Reynolds for their help in obtaining this material.

[10]This is the ratio of the sample resistivity at room temperature, ~313 °K, to that at 4.2 °K.

[11]P. M. Everett, following paper, Phys. Rev. B 6, 3559 (1972).

[12]The cutting solution used consisted of 13% concentrated nitric acid and 2% hydrofluoric acid in water.

[13]The angle of rotation was calibrated at room temperature by reflection of a focused light beam off a mirror attached to the tilt wheel. Very small and negligible unevenness in the teeth were observed. The reading at which the tilt wheel was aligned along the length of the sample holder, i.e., along the field, could not be determined in this way since differential thermal contraction would rotate the tilt wheel on cool down. However, this sample holder was also used in the investigation of Ref. 11, and the dHvA rotation patterns very accurately determined this dial reading.

[14]This solder has a work function very near that of copper thereby reducing thermoelectric effects to an acceptable level.

[15]Presentation of the data in this way makes the results independent of sample geometry.

[16]This even component was less than 1% of the TMR.

[17]The unusual case of a plane Fermi surface where open orbits exist for all field directions except the singular direction normal to the plane is not considered.

PHYSICAL REVIEW B VOLUME 6, NUMBER 10 15 NOVEMBER 1972

de Haas-van Alphen Studies in Zirconium*

P. M. Everett†
Department of Physics and Astronomy, Louisiana State University, Baton Rouge, Louisiana 70803

(Received 13 April 1972)

The de Haas–van Alphen effect has been studied in Zr in fields up to 57 kG. The five previously reported frequency branches have been observed as well as two new ones. The symmetry-axis frequency values have been determined with an uncertainty on the order of 0.1%, and the angular dependence of all the branches has been firmly established. It seems unlikely that any Fermi-surface model presently available can account for these results. All but one of the cyclotron masses associated with these oscillations have been measured at the symmetry axes. Except in one case these mass values are greater than the free-electron mass.

I. INTRODUCTION

The first study of the Zr Fermi surface was the de Haas–van Alphen (dHvA) investigation of Thorsen and Joseph[1] (TJ). They used the pulsed-field technique up to 190 kG and established the existence of five dHvA frequency branches. Since it was not clear to what degree and in what manner the d electrons contributed to the conduction process, they considered the nearly-free-electron model for fractional valence ranging from two through four and found that they could not fit their data to any reasonable distortion of it. Recently, Schirber,[2] as part of a study of the pressure dependence of the

Zr Fermi surface, measured the dHvA frequency values at the symmetry axes with improved precision but did not report the existence of any new branches.

Two band calculations have been performed for Zr. The first by Altmann and Bradley[3] (AB) used the cellular approach. The model of the Fermi surface they developed is fairly complex and contains sheets in the third through sixth bands. Their model is able to account in a rough way for all but one of the frequency branches observed by TJ. However, they assigned two of the extremal orbits to the same closed, simply connected sheet of the Fermi surface, and the corresponding frequency branches then would have to blend together. While the results of TJ tend to indicate that this is not the case, the scatter in the data of this early investigation was large enough such that no definite conclusions could be reached. The double-zone scheme was used by AB, but introduction of a spin-orbit energy gap at the hexagonal zone face would not affect comparison of the model with the dHvA data. The second band calculation was performed by Loucks[4] using the augmented-plane-wave method. This Fermi surface contained sheets in the third, fourth, fifth, and sixth bands and is able in a rough way to account for the existence of all the frequency branches observed by TJ. However, comparison of the angular dependences could not be made owing to the uncertainty in the experimental data, and the model predicts several oscillations that should be quite strong but have not been observed.

The present investigation measured the frequency branches seen by TJ with improved resolution and accuracy and extended the angular range of observation. Two new branches have been discovered and the angular dependences of all the branches firmly established. In addition, the symmetry axis values of the cyclotron masses of all but one of the branches have been measured.

II. EXPERIMENTAL PROCEDURE

The cutting of the samples used in this investigation was described elsewhere.[5] The dimensions of the samples were about 2 mm on each side by 6 mm long.

The dHvA effect was detected by the field-modulation technique in a 57-kG superconducting solenoid. A block diagram of the apparatus is shown in Fig. 1. The experimental arrangement was fairly standard and will be described only briefly. The modulation field was produced by a superconducting solenoid inserted into the lower tail of the experimental Dewar. This solenoid was capable of producing modulation amplitudes in excess of 1.5 kG; however, modulation fields in excess of 300 G caused the magnet to quench. This effectively limited detection to the second and fourth harmonics of the modulation frequency[6] which was always 100 Hz. The modulation amplitude was made proportional, to within 1%, to the magnetic field by an analog circuit called the modulation multiplier.[7] The field dependence of the detected amplitude then was independent of the detection scheme and proportional to the dHvA amplitude.[8] The sample was inserted into one of a pair of counterwound coils. Each coil had approximately 6000 turns of 0.04-mm-diam copper wire. The coils were not exactly bucked, and the twin-T filter was used to remove the residual signal at the modulation frequency. The dHvA oscillations were made periodic in time by sweeping the field inversely in time with a $1/H$ drive that has been described elsewhere,[9] and real-time filtering techniques were used to separate the various dHvA oscillations. The magnet current was read with a digital voltmeter which was calibrated with nuclear magnetic resonance (NMR) of Al^{27}. The procedures used to accurately determine the dHvA frequency values are described below.

The sample holder described in Ref. 5 was also used in this investigation. An expanded view of the lower section is shown in Fig. 2. The coil form b was turned from the same Epoxy as the rest of the lower section. The sample a was mounted on the end of an Epoxy rod with Duco cement and inserted into one of the counterwound coils. The coil form was then mounted in an aligned holder, and the sample was x-rayed. The maximum acceptable misorientation was $\frac{1}{4}°$. The coil form was placed in the tilt wheel, and the sample holder in the experimental Dewar. For the dHvA-frequency measurements the helium bath in the experimental Dewar was pumped to the lowest attainable temperature of 1.2 °K. For the cyclotron-mass measurements this bath was pressure regulated between 1.2 and 2.3 °K.

At the beginning of each run the sample was rotated continuously with the magnet at full field. The resulting field rotation pattern was used to very accurately locate the symmetry axis along the sample length. For the frequency determinations in the $(10\bar{1}0)$ and $(11\bar{2}0)$ planes, a field sweep of the dominant oscillation was made at this symmetry axis and the digital voltmeter readings recorded. Similar field sweeps were then made for all the dHvA frequencies at the various field directions. The number of oscillations in a given field interval was then compared to the corresponding number of oscillations of the dominant frequency at the symmetry axis. This was done for four overlapping field intervals on each field sweep. In this way each frequency value was measured relative to the value of the dominant-axis frequency entirely independently of the absolute magnet calibration . At the end of each run the symmetry-

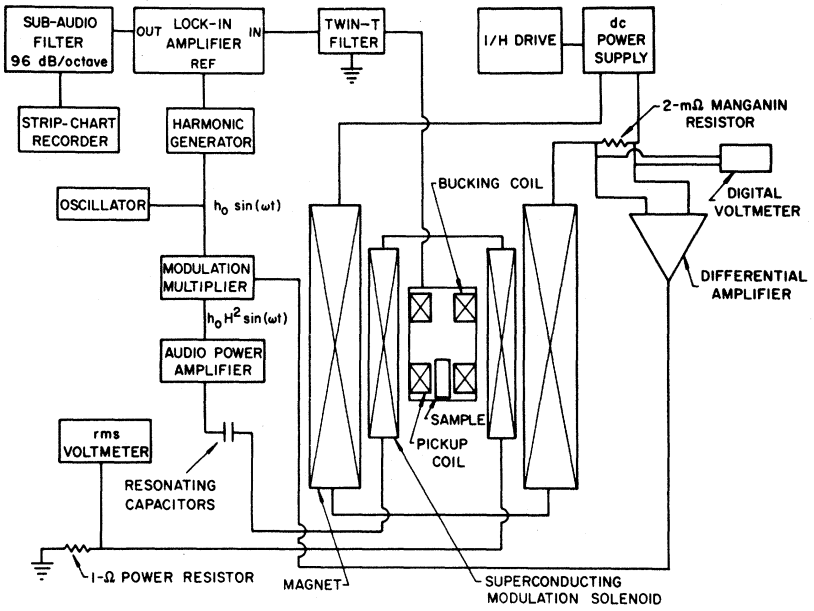

FIG. 1. Block diagram of the experimental arrangement. The Dewar system is not shown.

axis field sweep was repeated and no discrepancy was ever observed. At the beginning of this investigation and again at the end absolute values for the dominant axis frequency values were obtained with NMR calibration of the field. An unfiltered-field sweep was made at each axis. The sweeps covered a 20-kG interval, and the field was swept at a linear rate of 100 G/min. Then with the field still up the dHvA sample holder was removed and replaced by the NMR sample holder. The field was then swept at the same rate over the same range through some 20 resonances. The field was ramped back up and the process repeated to look for hysteresis; none was found. The digital voltmeter readings were found to be linear in field with a nonzero intercept that did not exceed 60 G. This was assumed to be due to trapped flux that remained pinned at high fields. As is discussed in the following section, the angular dependence of one frequency branch α was very well known in the basal plane. Therefore, in this plane a somewhat different frequency determination procedure was used. At the various field orientations in this plane the ratio of the desired frequency value to the α value was determined directly from each field sweep, and the known value was used to determine the desired value. This turned out to be more accurate than the comparison method. The uncertainties in the dominant axis frequency values are less than 0.1%. For those axis oscillations that formed good beat patterns with the dominant oscillation, the uncertainties are also no more than 0.1%. For those that did not and for the nonaxis frequency values the uncertainty rarely rises above 0.25%.

III. DE HAAS–VAN ALPHEN RESULTS

The collected dHvA results are shown in Fig. 3. The branches labeled α, β, γ, δ, and ϵ were seen by TJ. They are seen here somewhat extended in angular range and with improved resolution. The branches labeled ζ and η are new. The frequency values at the symmetry axes are listed in Table I with the results of TJ and Schirber.

The α branch varies smoothly and was observed throughout all three symmetry planes. The branch is dominant everywhere except in the vicinity of [0001]. The branch was covered with field sweeps spaced about 2° apart and with field rotation pat-

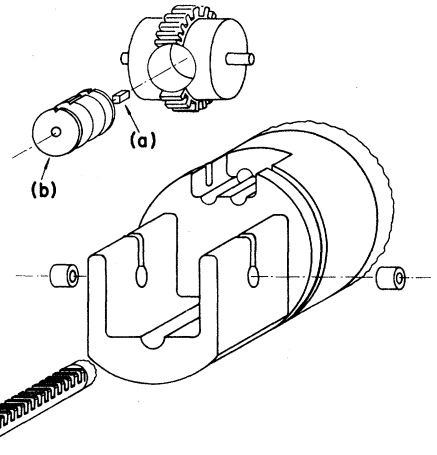

FIG. 2. Exploded view of the lower section of the sample holder: (a) sample; (b) coil form.

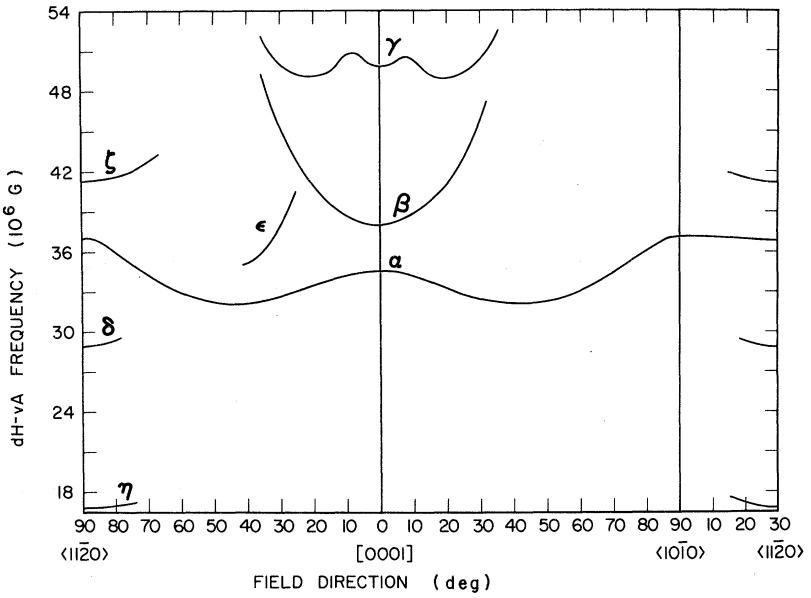

FIG. 3. Collected dHvA frequency values vs magnetic field direction.

terns in the (0001) and (10$\bar{1}$0) planes. The basal-plane rotation pattern gave a difference of 131 ± 2 kG in the frequency values at the two axes, and the field sweeps clearly indicate that the ⟨10$\bar{1}$0⟩ value is the larger. The rotation pattern waveform indicates that the branch has a shape very close to that of a cosine over a half-cycle. The small difference in the two symmetry-axis values and the smooth behavior between allow the α branch in this plane to be known quite precisely, and since the analysis of much of the other basal-plane data depends strongly on the α branch, these data are shown greatly expanded in Fig. 4. The solid line is the cosine curve fitted to the NMR calibrated ⟨10$\bar{1}$0⟩ value. The data points are the field-sweep values determined by the comparison method and do not deviate more than 0.06% from the curve. The field rotation pattern in the (10$\bar{1}$0) plane gave the minimum in the α branch 43.2° from [0001]. This rotation pattern was made with the sample that had the ⟨11$\bar{2}$0⟩ axis located along the pickup coil axis. The amplitude of the oscillation was strongest with the field located along the ⟨11$\bar{2}$0⟩ axis and became progressively weaker as the field was rotated out of the basal plane. It was, however, still observable, though barely, with the field along [0001]. This amplitude dependence is what would be expected from a Fermi-

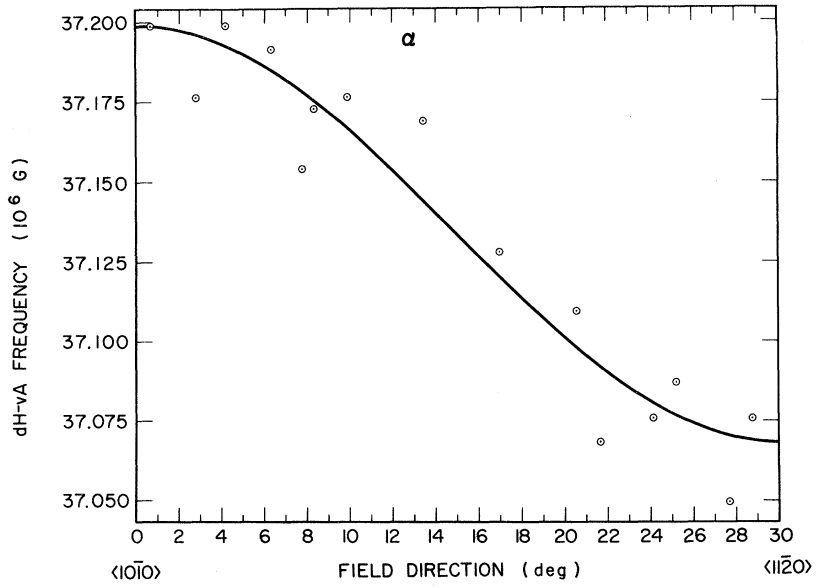

FIG. 4. Expanded plot of the α frequency values in the basal plane. The line is a half-cycle cosine fitted to the ⟨10$\bar{1}$0⟩ and ⟨11$\bar{2}$0⟩ values.

TABLE I. dHvA frequency values at the symmetry axes.

Oscillation	Axis	Frequency values (MG) Present investigation	Schirber	Thorsen and Joseph[a]
α	$\langle 10\bar{1}0\rangle$	37.22 ± 0.04	37.2	39.0
	$\langle 11\bar{2}0\rangle$	37.09 ± 0.04	37.0	37.4
	$\langle 0001\rangle$	34.58 ± 0.04	34.3	34.3
β	$\langle 0001\rangle$	38.00 ± 0.04	37.9	38.3
γ	$\langle 0001\rangle$	49.88 ± 0.05	51.0	50.3
δ	$\langle 11\bar{2}0\rangle$	28.99 ± 0.04	29.0	29.6
ξ	$\langle 11\bar{2}0\rangle$	41.25 ± 0.04		
η	$\langle 11\bar{2}0\rangle$	16.85 ± 0.03		

[a]Extracted from the plots in Ref. 1.

surface sheet for which the magnetic moment vector rotated approximately with the applied field.[10] In the $(11\bar{2}0)$ plane all the data were obtained by field sweeps. It was not felt that any additional useful information would be obtained by tracing this plane with a rotation pattern. The α data indicate that the branch exists on a closed sheet of the Fermi surface that supports only one extremal orbit. The shape of this branch indicates that the sheet is nearly spherical. It has some oblateness in the basal plane being pulled out somewhat more along $\langle 11\bar{2}0\rangle$ than along $\langle 10\bar{1}0\rangle$. It is as well pulled out somewhat more along [0001] than along the other two axes. Aside from the slight noncircular shape in the basal plane, this sheet has a shape somewhat akin to, although less exaggerated than, a child's top. To demonstrate this the sheet was assumed to be one of revolution about [0001], and the extremal cross sections of a prescribed shape were computer calculated and fit to the data. The fit was made to better than 1%, and the cross section of the resulting sheet is shown in Fig. 5(a). Since the α sheet is so close to one of revolution this shape must be very close to that of the true Fermi surface.

The β and γ results are shown in an expanded plot on Fig. 6, where the β branch is compared to a secant drawn through its [0001] value. The area formed by the intersection of a straight-sided cylinder of any cross section and a plane will increase as the secant with the angle between the cylinder axis and the normal to the plane. Since the β branch increases more rapidly than the secant in both symmetry planes, it would appear that this orbit encloses a waist or minimal extremal orbit on a sheet of the Fermi surface extending along the [0001] direction. The γ branch has a rather unusual angular dependence. In an attempt to determine some possible shapes for this section of the Fermi surface, the fitting technique for α was applied even though there is no reason to believe that this sheet has a near-circular cross section.[11] A fit to the data was obtained for the case in which γ was a central orbit, and this shape is shown in Fig. 5(b). The calculated extremal cross sections coincided with the experimental data and only began to have a noticeable deviation on the order of 2%, at angles greater than 30° from [0001]. This would be the expected result of a noncircular cross section. The data would seem to indicate that β and γ exist as maximal and minimal extremal orbits on the same sheet of the Fermi surface. There is not enough room within one Brillouin zone to attach a section of Fermi surface supporting the β orbit to the piece shown in Fig. 5(b). The investigation of Ref. 5 has ruled out any substantial number of carriers taking part in open orbit conduction. Therefore, an undulating cylinder does not seem to be a possibility, and if γ is a central orbit, β and γ must exist on different parts of the Fermi surface. The possibility of a noncentral γ orbit was also investigated with the fitting technique. In this case there was enough room, although barely, to fit both β and γ onto the same sheet of the Fermi surface within one zone. The fit to the γ data was as good as it was with the central case. The fit to the β data was better than the scatter in the experimental points. This Fermi surface is shown in Fig. 5(c). If the top and bottom were flat as indicated, a very strong basal-plane signal should be observed, unless the mass became anomalously large large, and none was. Only a trace of another oscillation, presumably β or γ, appeared in the vicinity of [0001] on the rotation pattern used to trace α in the $(10\bar{1}0)$ plane. This would indicate that β

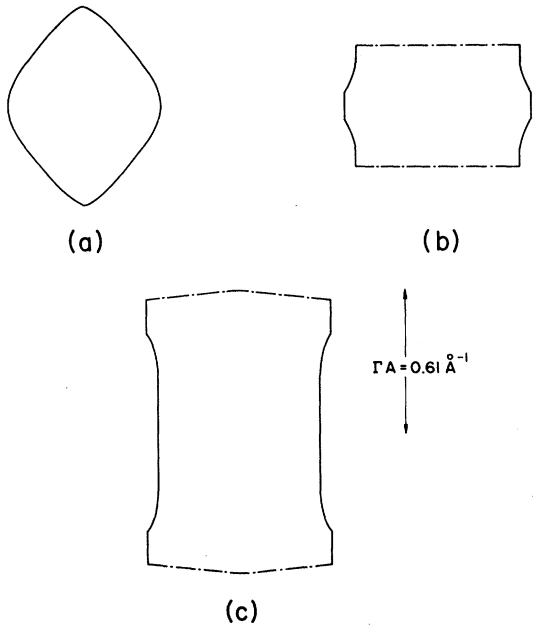

FIG. 5. Cross sections of surfaces of revolution fit to the dHvA results: (a) α; (b) central γ; (c) noncentral γ and central β. The half-height of the Brillouin zone, ΓA, is shown for comparison purposes.

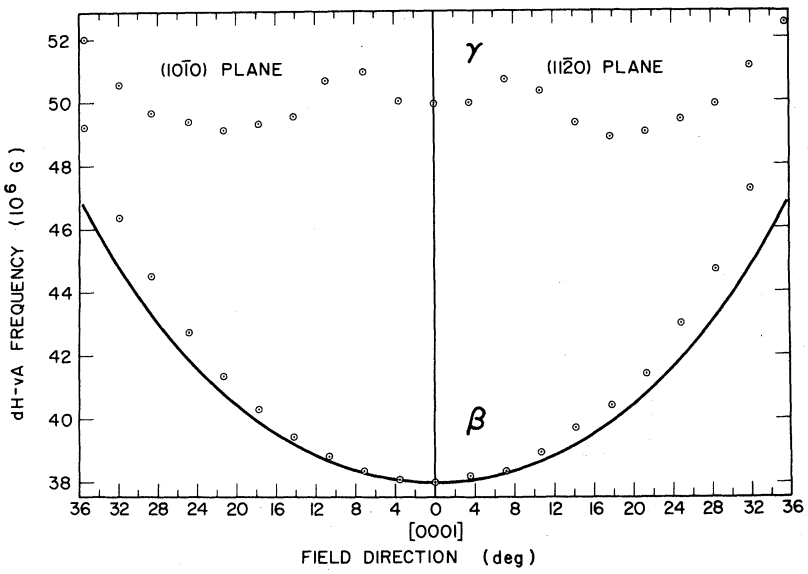

FIG. 6. Expanded plot of the β and γ data. The line is a secant fitted to the [0001] value.

and γ exist on a sheet or sheets of the Fermi surface that extend along [0001]. The magnetic moment vectors of these two oscillations then would be directed primarily along [0001] and perpendicular to the pickup coil axis.

Little can be said about the ϵ branch. It was traced both with field sweeps and rotation patterns. The amplitude of the signal did not cut off sharply with angle as would be expected for an extremal orbit that ran onto some protuberance on the Fermi surface. Rather, the amplitude decreased steadily at both ends of the branch until it was unobservable as would be expected from a continuously narrowing band of extremal orbits.

The δ branch is shown in Fig. 7 and compared to secant behavior. The electronic-filter ring proved to be more of a problem with this particular branch than for any other. The branch was observed at angles greater than those shown, but reliable frequency values could not be obtained. However, there is sufficient data to ensure that the δ branch exhibits secant behavior and that the orbit exists on a part of the Fermi surface that is cylindrically shaped and extended along $\langle 11\bar{2}0 \rangle$.

The η data are shown in an expanded fashion and compared to the secant in Fig. 8. This branch increases more rapidly than the secant in the basal plane and less rapidly in the $(10\bar{1}0)$ plane. A section of Fermi surface whose cross section in the basal plane is concave and whose cross section in

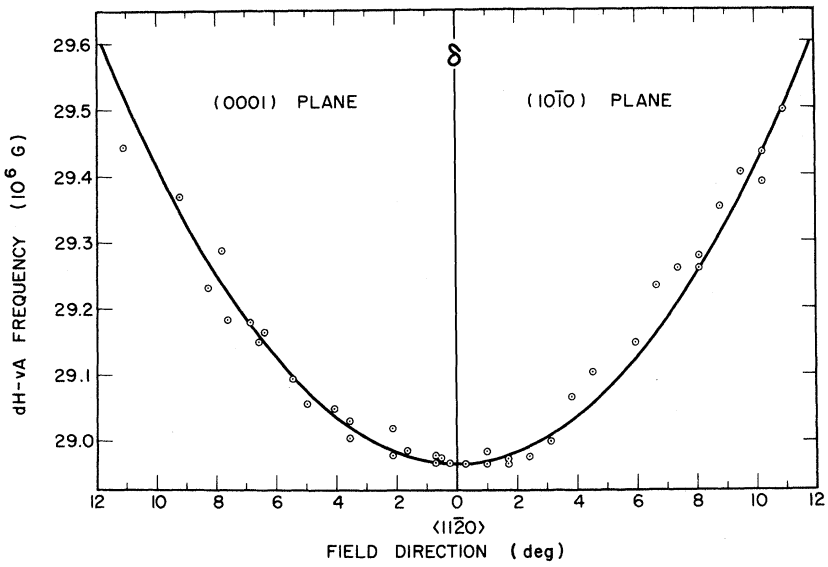

FIG. 7. Expanded plot of the δ data. The line is a secant fitted to the $\langle 11\bar{2}0 \rangle$ value.

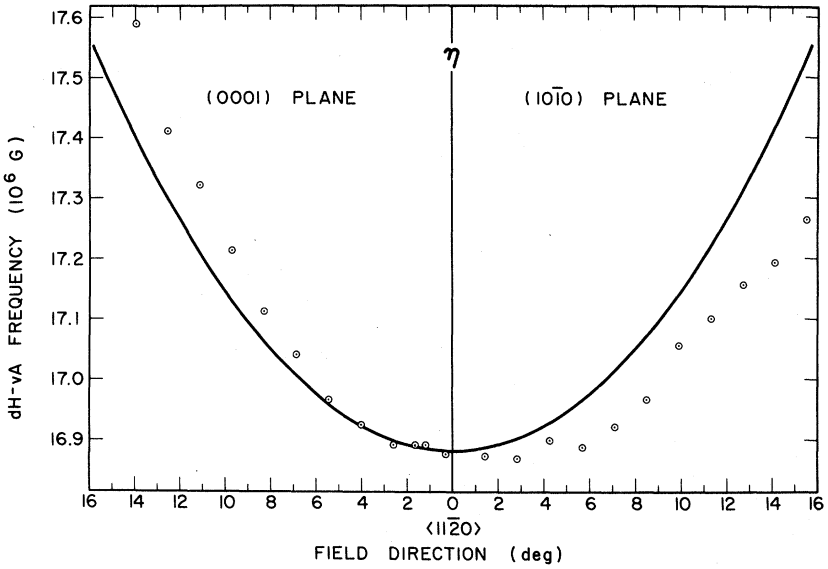

FIG. 8. Expanded plot of the η data. The line is a secant fitted to the $\langle 11\bar{2}0\rangle$ value.

the $(10\bar{1}0)$ plane is convex would support such an orbit. Such a piece of Fermi surface might be considered to be canoe shaped.

The ζ data are shown in a similar fashion in Fig. 9. Since the branch increases less rapidly than the secant in both planes, it would appear that this oscillation comes from a maximal extremal orbit, or bump, on a section of the Fermi surface extending along $\langle 11\bar{2}0\rangle$.

IV. CYCLOTRON MASSES

The cyclotron masses were measured from the temperature dependence of the amplitudes of the dHvA oscillations. The number of temperature points used ranged from five to nine. Even with filtering no oscillation could be completely isolated, and the best that could be obtained were reasonably clean two-oscillation beat patterns. When the beat pattern could be made sufficiently weak, the mass-oscillation method[12] was used to determine the mass of the dominant oscillation. When this was not the case, the sum and difference of the node and antinode amplitudes were used to determine the masses of both oscillations. Each mass value was determined by both methods from data obtained on at least two runs, and all values are consistent. The details of the two mass-determination methods are described in the Appen-

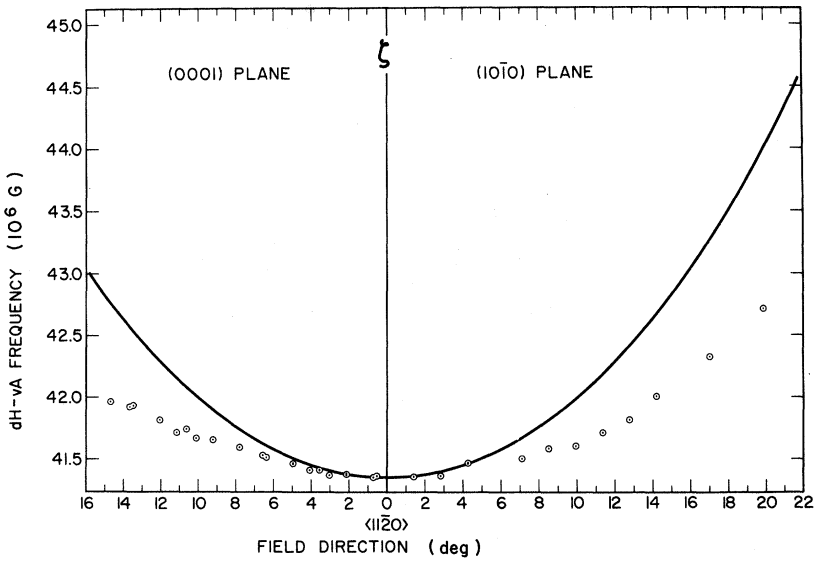

FIG. 9. Expanded plot of the ζ data. The line is a secant fitted to the $\langle 11\bar{2}0\rangle$ value.

dix.

Mass values were obtained for all oscillations at the symmetry axes except η. The low amplitude of this oscillation combined with the filter ring problems at low frequencies prevented a reliable value from being obtained. Values were also obtained for the α and ϵ masses at a representative field orientation in the $(10\bar{1}0)$ plane. If β and γ do exist on a closed simply connected sheet of the Fermi surface, a large cyclotron mass could explain the absence of this oscillation for the field directed near the basal plane. An attempt was made to trace the β and γ mass values out from [0001] to see if they increased significantly. Unfortunately, the oscillations became too weak to obtain reliable values.

The mass values obtained are listed in Table II. The values are all fairly substantial with apparently only the α mass away from the basal plane dropping below the free-electron mass. This cannot be commented upon in much detail without an accurate picture of the Zr band structure. However, the bands are apparently fairly flat, and one is led to think that this is most likely due to the d character that the bands must exhibit.

V. FERMI-SURFACE MODELS

Thorsen and Joseph have shown that no reasonable distortion of the free-electron model can account for the experimental data. The models of AB and of Loucks will be discussed in turn.

As they mentioned in their original paper, AB cannot account for the ϵ branch and its limited angular range. Their model also assigns the α and β branches to the same closed sheet of the Fermi surface as minimal and maximal extremal orbits, respectively. The two branches then would necessarily have to blend together as the field is rotated toward the basal plane. This does not happen,[13] and β is clearly a minimal rather than maximal extremal orbit. There is no piece of the AB Fermi surface that can account for the cylindrical shape of the δ orbit, and the model does not contain sheets of the appropriate size and shape to account for the η and ζ oscillations. Also several oscillations are predicted by this model, some of which should have substantial amplitudes, that have not been observed.

TABLE II. Cyclotron-mass values in units of the free-electron mass.

Oscillation	Orientation	Mass
α	$\langle 10\bar{1}0\rangle$	1.35 ± 0.04
α	$\langle 11\bar{2}0\rangle$	1.34 ± 0.04
α	$\langle 0001\rangle$	0.95 ± 0.03
β	$\langle 0001\rangle$	1.14 ± 0.02
γ	$\langle 0001\rangle$	1.45 ± 0.15
δ	$\langle 11\bar{2}0\rangle$	1.75 ± 0.15
ζ	$\langle 11\bar{2}0\rangle$	1.83 ± 0.05
α	36.1° from [0001] toward $\langle 11\bar{2}0\rangle$	0.85 ± 0.02
ϵ	36.1° from [0001] toward $\langle 11\bar{2}0\rangle$	1.39 ± 0.05

The Loucks model adequately accounts for the α oscillation with the third-zone hole sheet,[14] and the fourth-zone hole sheet could be distorted to account for β and γ. In his double-zone scheme calculation, Loucks originally connected the third- and fourth-zone sheets by a narrow neck. This neck was subsequently pinched off by Loucks to create the α sheet in the third zone and a corresponding closed sheet in the fourth zone. If the fourth-zone sheet were stretched out almost to the hexagonal-zone face and if the central section were pushed in to create a waist, the fourth-zone sheet could well have a shape similar to that shown in Fig. 5(c). Loucks's model predicts an electron sheet in the fifth zone. This sheet apparently can support three $\langle 11\bar{2}0\rangle$ centered extremal orbits. One, which runs on the outside of two adjacent pillars and across the two connecting arms and is definitely maximal, was assigned to δ by Loucks. Loucks's calculated frequencies are generally about 40% larger than the experimental results, and this orbit has about the right size for ζ. Another is the orbit that runs up one side of a vertical pillar and down the other side of the same pillar. With some adjustment in size and shape to insure that it is extremal, this orbit might correspond to the concave-convex η orbit. It would appear from Loucks's sketch of his Fermi surface that this portion has the appropriate concaveness. The needed convexness could be accomplished by putting a hump on each "duck's beak" at the top and bottom of the pillars, a reasonable distortion. The third $\langle 11\bar{2}0\rangle$ centered orbit on Loucks's fifth-zone sheet encircles the hole between two pillars and an upper and a lower arm. The size of this orbit would lie between the other two and could be appropriate for δ. However, the pillars would have to be rather severely and exactingly distorted to give this orbit the required cylindrical shape. Loucks assigned the ϵ orbit to run over the tops of two connecting arms on the upper toruslike ring on the fifth band, down the outside of two pillars and across the bottom of a connecting arm on the lower ring. With the present assignment of orbits, the size of the ϵ orbit would require that ϵ is rather the corresponding orbit on the inside of the multiply connected sheet running along the bottom of the two upper arms down the inside of the pillars and over the top of the lower arm. This orbit would then be the continuation of δ on the other side of the hole in the upper ring. The slopes of the two branches certainly indicate that this may be the case. However, the outside extremal orbit should certainly exist and, it would appear, be much stronger than the inside orbit,

but it has not been observed. Loucks's model predicts other extremal orbits on the fifth-zone sheet that should produce quite strong and detectable signals. One encircles the connecting arms with the field along $\langle 10\bar{1}0\rangle$, another encircles a pillar with the field along $\langle 10\bar{1}0\rangle$ by running through the holes in the upper and lower rings, and a third encompasses a pillar with the field along [0001]. Serious searches were made for these oscillations, but they were not seen. The band shown by Loucks to be producing the pillar is particularly flat. Since the cyclotron mass amounts to the averaged slope of the band over the orbit, the absence of this oscillation could well be explained by a large mass value. Since the connecting arm does not lie in a symmetry plane, the bands producing it are not shown by Loucks, but a similar explanation of band flatness is possible. However, within this assignment of the orbits to the Loucks model, the outside portions of the pillars and arms are sampled by the ζ orbit and the inside portions by the δ and ϵ orbits. So if the orbits encircling the pillars and arms are not seen owing to band flatness, it would seem most reasonable that the ζ, δ and or ϵ oscillations would be unobservable for the same reason. The absence of the $\beta-\gamma$ oscillation for the field in the basal plane also seems difficult to explain except through an anomalously large mass value. The model also contains sixth-zone ellipsoidal electron sheets that have not been observed.

It is not obvious how the AB model can be modified to fit the experimental results. It is possible to modify the Loucks model to fit these results. However, the modifications are fairly severe, and the circumstance of large mass values must be repeatedly called upon to explain the absence of oscillations that from the widths of the bands of orbits would be expected to be quite strong. While so many large mass values may indeed be the case in this transition metal, it is apparent that if the Loucks model is basically correct it will have to undergo considerable reworking to produce a true picture of Zr. Perhaps one of the most disturbing aspects of the Loucks model is the δ oscillation. In order to fit this shape orbit to Loucks's H centered sheet, the pillars would have to be four-sided with the two interior sides being straight and forming a right angle, a rather unusual shape. However, such a cylindrically shaped section of Fermi surface would occur naturally as connecting arms on a hexagonally shaped Γ or A centered sheet.

ACKNOWLEDGMENTS

The author would like to express his sincere appreciation to Professor C. G. Grenier for many helpful and stimulating discussions and for suggesting fitting the data to surfaces of revolution. Thanks are due as well to Professor R. G. Goodrich for his help during the early stages of this investigation, to Dr. C. R. Crosby for his generous assistance with the computer fitting, and to Professor J. C. Kimball for an enlightening discussion.

APPENDIX: EXTRACTION OF THE CYCLOTRON MASSES

In determining the cyclotron masses the Lifshitz-Kosevitch (LK)[15] expression for the dHvA amplitude was assumed to be applicable. It was not possible to completely isolate any oscillation, and the cyclotron masses had to be extracted from two oscillation beat patterns. Depending on the strength of the beat, two methods were used to determine the mass values. In both cases the LK expres-

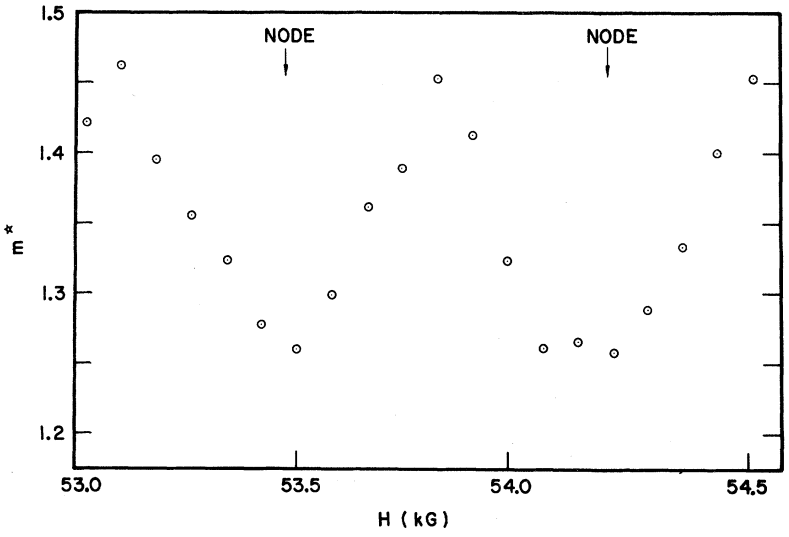

FIG. 10. Apparent mass values of α at $\langle 11\bar{2}0\rangle$ obtained from a weak-beat pattern by the method dicussed in the text.

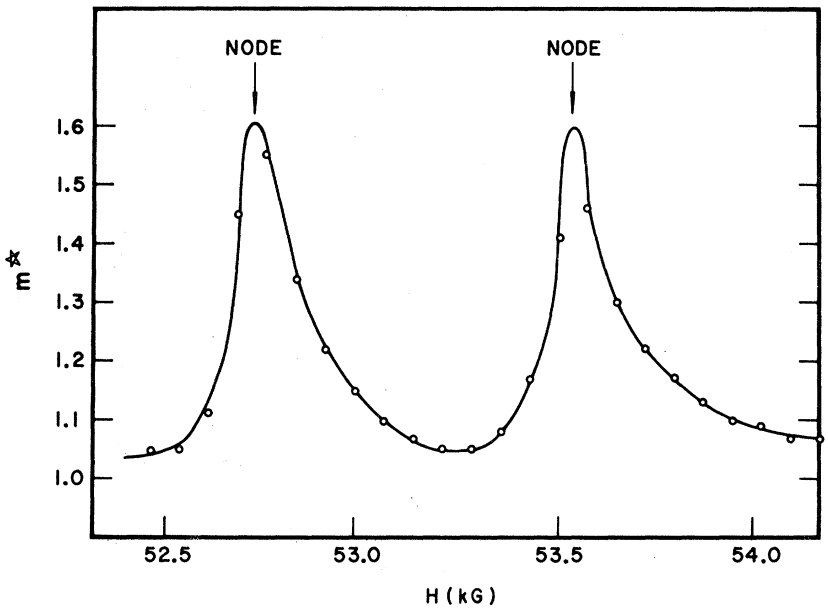

FIG. 11. Apparent mass values of β at [0001] obtained from a strong-beat pattern.

sion for the amplitude of a single dHvA oscillation was assumed and the cyclotron mass value determined by making a self-consistent, or iterative, least-squares fit of this expression to the data.

The first was the mass oscillation method described in Ref. 10. and was used only for sufficiently weak beat patterns. If the presence of the recessive oscillation is ignored, the apparent mass of the dominant oscillation measured from the temperature dependence of successive oscillations in the beat pattern is found to oscillate with the period of the beat. Two points need to be made that were not made in Ref. 10. From Eq. (4) of Ref. 10:

$$m_{1a} = m_{1t} - \eta\left(\frac{B}{k}\,\frac{n\Sigma Tf - \Sigma T\Sigma F}{n\Sigma T^2 - (\Sigma T)^2}\right) , \tag{1}$$

$$f = \exp\left(\frac{-k(m_{2t} - m_{1t})(T+X)}{B}\right)\,\frac{1-\exp(-2km_{1t}T/B)}{1-\exp(-2km_{2t}T/B)} . \tag{2}$$

The symbols have their usual significance, with m_{1t} and m_{2t} referring to the masses of the dominant and recessive oscillations, respectively. η is the phased ratio of the amplitudes of the two oscillations and oscillates between positive and negative extremes with the period of the beat. The summations are made over the n temperature points. Thus the apparent or measured mass value m_{1a} oscillates with the period of the beat since the quantity in the large parentheses of Eq. (1) varies only slowly with field. This term will be positive if f is an increasing function of T and negative if f is a decreasing function of T. If f increases with T, then η is negative at the node of the beat pattern, and m_{1a} will have its minimum value. The opposite will be true if f decreases with T. Within the limit of the approximations made, f will increase with T if $m_{1t} > m_{2t}$ and decrease if $m_{1t} < m_{2t}$. Thus not only can the mass of the dominant oscillation be determined from the mean of the two extremes of m_{1a}, but also whether the mass of the recessive oscillation is greater or less than the mass of the dominant oscillation. The apparent mass values obtained for α in this way from a weak $\alpha - \zeta$ beat pattern at $\langle 11\bar{2}0\rangle$ are shown in Fig. 10. The distortion from a good sine wave is caused by the presence of some δ oscillation. Since the apparent mass minimums occur at the node of the beat pattern, the ζ mass must be greater than the α mass which it is. It should also be pointed out that there is some inherent danger in this method of mass extraction. Figure 11 shows the apparent mass values extracted from an $\beta - \alpha$ beat at [0001] in which the α amplitude is 43% of the β amplitude, far greater than the approximations allow. At this axis the β mass is 1.14 free-electron masses, a value that is not apparent from these data.

The second method of mass extraction used was to draw an envelope around the beat pattern. The antinode amplitude was then projected to the value it would have had if it had occurred at the node field. The node and antinode amplitudes were then added and subtracted to give the amplitudes of the individual oscillations, and the two mass values were determined independently.

*Work performed under the auspices of the U. S. Atomic Energy Commission and is AEC Report No. ORO-3087-50.

†Present address: Department of Physics and Astronomy, University of Kentucky, Lexington, Kentucky 40506.

[1]A. C. Thorsen and A. S. Joseph, Phys. Rev. 131, 2078 (1963).

[2]J. E. Schirber, Phys. Letters 33A, 172 (1970).

[3]S. L. Altmann and C. J. Bradley, Phys. Rev. 135, A1253 (1964); Proc. Phys. Soc. (London) 92, 764 (1967).

[4]T. L. Loucks, Phys. Rev. 159, 544 (1967).

[5]P. M. Everett, preceding paper, Phys. Rev. B 6, 3553 (1972).

[6]Only even harmonics were detected since the push-pull audio amplifier tended to concentrate the harmonic distortion in the odd harmonics.

[7]This was a simple circuit made up of operational amplifiers and hybrid multipliers. For this purpose the magnetic field was assumed to be proportional to the magnet current.

[8]A. Goldstein *et al.*, Rev. Sci. Instr. 36, 1356 (1956).

[9]P. M. Everett, Rev. Sci. Instr. 43, 753 (1972).

[10]For a sheet of the Fermi surface that was spherical, the magnetic moment vector would always lie along the direction of the applied field.

[11]The fact that the γ branch rises up more and dips down less in the $(10\bar{1}0)$ plane is what would be expected from a sheet that was nearly hexagonal or triangular in cross section.

[12]P. M. Everett, Cryogenics 10, 314 (1970).

[13]If this were the case, the blending of the two orbits would have been directly observed in the rotation pattern that traced α throughout the (1010) plane.

[14]A very rough estimate from Loucks's energy bands of the band-structure mass for the α orbit lying in the basal plane yielded a value 16% less than the measured cyclotron-mass value, and this would correspond to a reasonable amount of many-body mass enhancement. The author would like to thank Professor J. C. Kimball for suggesting and making this estimate.

[15]I. M. Lifshitz and A. M. Kosevitch, Zh. Eksperim. i Teor. Fiz. 29, 730 (1955) [Sov. Phys. JETP 2, 636 (1956)].

PHYSICAL REVIEW B VOLUME 6, NUMBER 10 15 NOVEMBER 1972

Fermi Surface of Mg under Hydrostatic Pressure*

G. M. Beardsley, J. E. Schriber, and J. P. Van Dyke
Sandia Laboratories, Albuquerque, New Mexico 87115

(Received 24 March 1972)

We report the effect of hydrostatic pressure on several cross-sectional areas of the Fermi surface of Mg. Pressure derivatives were obtained using the fluid-He phase-shift technique. The results differ significantly from the predictions of the free-electron model but are described quite well by a simple local-pseudopotential model.

I. INTRODUCTION

The Fermi surface of Mg has been studied in great detail by a variety of techniques including, in particular, magnetoacoustic[1] and de Haas–van Alphen[2,3] (dHvA) studies. The results are in general agreement with the free-electron construction[4] so that pseudopotential descriptions might be expected to be successful as model descriptions for Mg. Kimball, Stark, and Mueller[3] (KSM) fitted experimental data to pseudopotential models and concluded that a nonlocal description was required to achieve quantitative agreement with observation. Recent work[5,6] has shown that pressure studies of the Fermi surface can provide a fairly incisive test of a given pseudopotential model. The purpose of this paper is to report measurements of Fermi-surface cross sections as a function of hydrostatic pressure for comparison with the predictions of various model descriptions.

The Fermi surface of Mg consists of several sheets in the first four bands. Representations of these sheets have been presented many times in the literature so the reader is referred to the figures in Refs. 2 and 3. We have employed the nomenclature of KSM throughout. Here μ denotes cross sections associated with the second-band hole surface called the "monster," and λ and γ denote cross sections associated with the third-band electron sheets called the "lens" and "cigar," respectively. The subscripts 1 and 2 indicate whether the applied field is in the $(10\bar{1}0)$ or $(11\bar{2}0)$ plane. The superscripts number the cross sections in a given plane in order of increasing size. We will be concerned primarily with several of the second-band monster orbits and with third-band lens and cigar orbits. Although this is not a complete set of observable frequencies, we feel the six or seven orbits considered adequately represent both the normal volume and pressure behavior of the Fermi surface of Mg. Section II outlines briefly our experimental procedures. Section III describes a local-pseudopotential model that provides as satisfactory a fit to the normal-volume Fermi surface as does the nonlocal model described by KSM. This local model yields pressure derivatives for